

Autoregressive Speech Synthesis without Vector Quantization

Lingwei Meng^{1*} Long Zhou^{2†} Shujie Liu² Sanyuan Chen^{*} Bing Han² Shujie Hu¹
Yanqing Liu² Jinyu Li² Sheng Zhao² Xixin Wu¹ Helen Meng¹ Furu Wei²

¹The Chinese University of Hong Kong

²Microsoft Corporation

Abstract

We present MELLE, a novel continuous-valued tokens based language modeling approach for text to speech synthesis (TTS). MELLE autoregressively generates continuous mel-spectrogram frames directly from text condition, bypassing the need for vector quantization, which are originally designed for audio compression and sacrifice fidelity compared to mel-spectrograms. Specifically, (i) instead of cross-entropy loss, we apply regression loss with a proposed spectrogram flux loss function to model the probability distribution of the continuous-valued tokens. (ii) we have incorporated variational inference into MELLE to facilitate sampling mechanisms, thereby enhancing the output diversity and model robustness. Experiments demonstrate that, compared to the two-stage codec language models VALL-E and its variants, the single-stage MELLE mitigates robustness issues by avoiding the inherent flaws of sampling discrete codes, achieves superior performance across multiple metrics, and, most importantly, offers a more streamlined paradigm. See <https://aka.ms/melle> for demos of our work.

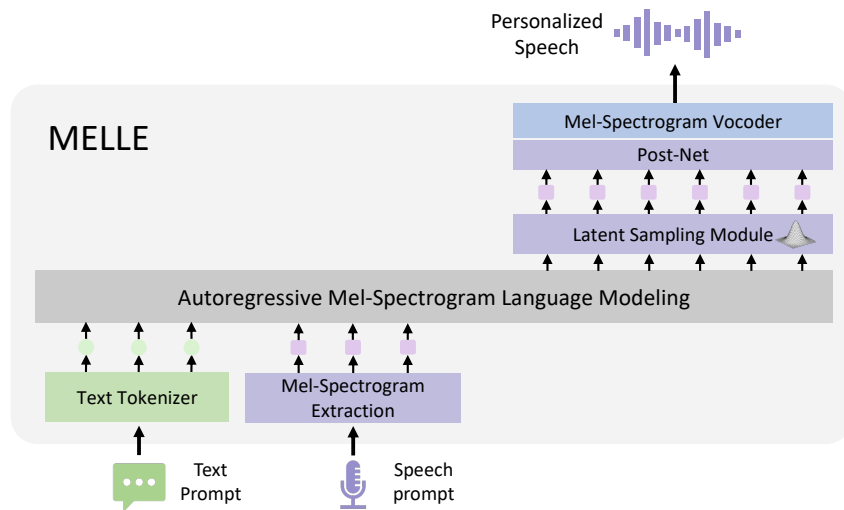


Figure 1: The overview of MELLE. Unlike discrete-valued tokens based language modeling approaches, MELLE generates the continuous variational mel-spectrogram conditioned on textual and acoustic prompts, using a single-stage decoder-only model as its foundational structures, coupled with the Latent Sampling Module.

*Work done during an internship at Microsoft Research Asia.

†Corresponding author.

1 Introduction

The objective of next-token prediction, which involves predicting the next discrete token based on the previous tokens as condition, is foundational to the recent progress observed in autoregressive large language models (LLMs) [Brown et al., 2020, OpenAI et al., 2023]. Recently, the success of LLMs in natural language processing (NLP) tasks has encouraged the exploration of autoregressive language modeling approaches in audio synthesis fields [Borsos et al., 2022, Wang et al., 2023]. Neural codec language models, exemplified by VALL-E [Wang et al., 2023] and VALL-E X [Zhang et al., 2023], reveal the potential of such principle in the zero-shot text-to-speech (TTS) task via leveraging large-scale multi-lingual multi-speaker multi-domain training corpus. Unlike traditional TTS systems that rely heavily on complex and multi-step pipelines, they utilize a decoder-only approach to predict neural codec codes, which are discrete tokens encoded from continuous waveforms leveraging neural codec models [Zeghidour et al., 2021, Défossez et al., 2023].

Although achieving impressive naturalness and diversity in synthesized audios, VALL-E and its variants are plagued by following several drawbacks. First, neural codec codes, originally designed for audio compression, exhibit lower fidelity compared to the well-established mel-spectrogram [Puvvada et al., 2024]. This phenomenon is also observed in the field of graphics, where the reconstruction quality of vector-quantized tokenizers typically lags behind that of their continuous-valued counterparts [Rombach et al., 2022, Huang et al., 2023, Li et al., 2024a]. Second, the codec language model VALL-E suffers from robustness issues stemming from its random sampling strategy, which is inherited from text language model for selecting discrete tokens. This issue is more pronounced with acoustic tokens as opposed to textual ones due to the greater similarity among consecutive codec codes, which can lead to continuous stretches of silence or persistent noise [Wang et al., 2023, Song et al., 2024]. Third, neural codec language models typically necessitate a complicated two-pass decoding process, involving an autoregressive (AR) model for generating coarse primary audio tokens, followed by a non-autoregressive (NAR) model to iteratively predict the rest multiple codebook codes for refinement. This multi-step procedure compromises inference efficiency, leading to increased computational demands and doubled storage requirements.

To address the limitations associated with discrete tokens based codec language models, we are re-thinking the potential of continuous speech representations and aim to determine whether continuous-valued tokens can supplant discrete-valued tokens within the paradigm of autoregressive speech synthesis models. The successful implementation of the autoregressive model without discrete vector quantization faces two key challenges.

- **How to set training objective for continuous representation?** The continuous space significantly differs from that of vector-quantized tokens, for which autoregressive language models typically adopt a next-token prediction objective, with cross-entropy loss to measure the discrepancy between the predicted distribution and the ground truth.
- **How to enable sampling mechanism in continuous space?** The sampling strategy is a critical component in both text generation and speech synthesis systems, as it introduces diversity into the output and enhances the generalization ability. However, continuous-valued tokens based models can not employ top-p random sampling method used in discrete codec language models.

In this work, we propose a continuous mel-spectrogram¹ based autoregressive language model (called MELLE) for text-to-speech synthesis, as illustrated in Figure 1. MELLE is a robust single-pass zero-shot TTS model which autoregressively predicts mel-spectrogram frames based on previous mel-spectrogram and text tokens, thereby avoiding the inherent flaws associated with sampling discrete codec codes. The mel-spectrogram is then converted into waveform utilizing an off-the-shelf vocoder. In response to the aforementioned challenges, we first substitute cross-entropy loss with regression loss and introduce a spectrogram flux loss to promote variation of predicted mel-spectrograms and eliminate repetition issues. Second, we design a latent sampling module, derived from variational inference, functions as a sequence sampling strategy thereby enhancing the diversity of the generated audio samples. As an option, by adjusting the reduction factor, MELLE can predict multiple frames at one step and accelerate inference, thereby further alleviating the robustness issues associated with long-sequence modeling and maintaining satisfactory performance.

¹We leave the exploration of other continuous representations, such as VAE latent hidden states, for future research endeavors.

We conducted evaluations of our MELLE on both the large-scale 50K-hour Libriheavy [Kang et al., 2024] training dataset and the relatively small 960-hour LibriSpeech [Panayotov et al., 2015] training dataset. Following recent works, we use LibriSpeech test-clean set for zero-shot TTS evaluation. Experimental results demonstrate that the proposed MELLE is on par with VALL-E 2 [Chen et al., 2024] in objective metrics, and surpasses VALL-E 2 in subjective metrics. It also outperforms previous neural codec language models, including VALL-E and its other variants, achieving superior performance across multiple metrics that reflect naturalness, robustness, similarity, and inference efficiency. Specifically, MELLE surpasses the ground truth audios in WER (1.47% vs. 1.61%), achieving a 47.9% relative reduction in WER compared to VALL-E and an 8.1% reduction compared to VALL-E 2 on the continuation inference task for zero-shot TTS. For subjective evaluations, MELLE is more favorably received by human listeners than previous models, achieving comparable performance to the original ground truth in terms of MOS (4.20 vs. 4.29) and CMOS (-0.032 for ours vs. ground truth), and an even higher SMOS (4.40 vs. 3.94) than the ground-truth speech.

2 Related Work

2.1 Traditional TTS

Traditional speech synthesis methods can be categorized concatenative systems, parametric systems, and end-to-end neural systems. Concatenative TTS systems deconstruct original audio waves into smaller segments and then reassembles them using algorithms like Viterbi, followed by signal processing techniques, to create new audio waves [Hunt and Black, 1996, Black and Taylor, 1997]. Parametric TTS systems convert speech waves into spectrograms, utilizing acoustic parameters such as fundamental frequency and duration to synthesize new audio outputs [Zen et al., 2013, Tokuda et al., 2013]. With the rapid development of neural networks, end-to-end neural TTS systems are proposed to simplify previous speech synthesis pipeline via a single neural network, eliminating the need for the production of these linguistic and acoustic features [Wang et al., 2017, Li et al., 2019, Ren et al., 2019].

The advanced end-to-end neural TTS models, such as Tacotron [Wang et al., 2017], TransformerTTS [Li et al., 2019], and FastSpeech [Ren et al., 2019], usually generate mel-spectrograms directly from texts, then synthesize the audio results from the mel-spectrogram by a vocoder such as WaveNet [Oord et al., 2016]. TransformerTTS employs Transformer-based encoder-decoder network as the main framework to replace RNN structures in Tacotron. FastSpeech further improve the speech quality and decoding efficiency using the non-autoregressive generation model with a duration module. These model are trained on small-scale, clean, single-speaker or few-speaker dataset, such as LJSpeech [Ito and Johnson, 2017] and LibriTTS [Zen et al., 2019]. Our MELLE leverages the well-established mel-spectrogram as the intermediate representation, however, it differs significantly in two key aspects: (1) we adopt decoder-only network as foundational structure with improved methods, such as variational inference and spectrogram flux loss, (2) MELLE is capable of zero-shot TTS via training on large-scale speech-text paired data, like Libriheavy [Kang et al., 2024].

2.2 Zero-Shot TTS

Motivated by the zero-shot and in-context learning capabilities of large language models (LLMs) on natural language processing (NLP) tasks [OpenAI et al., 2023, Touvron et al., 2023], various research works are proposed to address zero-shot TTS through a language modeling approach [Wang et al., 2023, Zhang et al., 2023, Jiang et al., 2023]. VALL-E [Wang et al., 2023] first regards TTS tasks as a conditional language task, which utilizes neural codec codes as intermediate representation instead of mel-spectrogram, then uses a codec decoder to recover the waveform from predicted codec codes. VALL-E employs two-stage modeling method, with an autoregressive model for generating coarse audio tokens, followed by a non-autoregressive model to iteratively predict multi-codebook codes for refinement. VALL-E X [Zhang et al., 2023] extends VALL-E into multi-lingual scenario to support zero-shot cross-lingual speech synthesis and speech-to-speech translation. Mega-TTS [Jiang et al., 2023] proposes to disentangle the multiple attributes in speech, such as content, timbre, prosody, and phase attributes, then model each of them according to their intrinsic properties with a language modeling approach. ELLA-V [Song et al., 2024], RALL-E [Xin et al., 2024], and VALL-E R [Han et al., 2024] aims to improve robustness and stability of VALL-E via additional fine-grained speech-text alignment information. BASE TTS [Łajszczak et al., 2024] employs discrete tokens derived from

WavLM [Chen et al., 2022] and scales the codec language model to larger parameters and training data. Seed-TTS [Anastassiou et al., 2024] replaces NAR model in VALL-E with a diffusion model, which generates continuous speech representations according generated speech tokens from AR stage. In parallel to our work, VALL-E 2 [Chen et al., 2024] shares the same architecture as VALL-E but employs a repetition-aware sampling strategy that promotes more deliberate sampling choices.

Other studies have investigated fully non-autoregressive approaches to increase the speed of model inference. For instance, SoundStorm [Borsos et al., 2023] adapts a parallel, non-autoregressive, confidence-based decoding scheme for the generation of codec codes. StyleTTS 2 [Li et al., 2024b] and NaturalSpeech 3 [Ju et al., 2024] use diffusion model to achieve better TTS synthesis. Voicebox [Le et al., 2024] and Audiobox [Vyas et al., 2023] employ non-autoregressive flow-matching based models for transcript-guided speech generation. Recently, E2 TTS [Eskimez et al., 2024] presents a fully non-autoregressive TTS systems consisting of flow-matching-based mel-spectrogram generator trained with the audio infilling task, and a vocoder. Different previous works, MELLE leverages continuous-valued tokens based autoregressive language modeling approach with variational inference for text-to-speech synthesis.

3 MELLE

3.1 Problem Formulation: Mel-Spectrogram Language Modeling

This study regards zero-shot TTS as an autoregressive mel-spectrogram language modeling task. Instead of predicting highly-compressed neural codec codes like VALL-E and its variants, MELLE directly predicts continuous mel-spectrograms which are then converted to waveforms with an off-the-shelf vocoder. Taking well-established mel-spectrogram as the training target, it strives to achieve higher fidelity and naturalness.

Given an audio sample with byte-pair-encoded (BPE) text content $\mathbf{x} = [x_0, x_1, \dots, x_{L-1}]$, MELLE is optimized to predict the mel-spectrogram $\mathbf{y} = [\mathbf{y}_0, \mathbf{y}_1, \dots, \mathbf{y}_{T-1}]$ extracted from the corresponding audio. Specifically, at each autoregressive step, MELLE is expected to predict the next mel-spectrogram frame \mathbf{y}_t conditioned on the text prompt \mathbf{x} and the previous generated mel-spectrograms $\mathbf{y}_{<t}$, which is equivalent to maximizing the following distribution:

$$p(\mathbf{y} | \mathbf{x}; \theta) = \prod_{t=0}^{T-1} p(\mathbf{y}_t | \mathbf{y}_{<t}, \mathbf{x}; \theta) \quad (1)$$

where $\mathbf{y}_{<t}$ denotes $[\mathbf{y}_0, \mathbf{y}_1, \dots, \mathbf{y}_{t-1}]$ and θ represents the parameters of MELLE.

Inspired by previous neural TTS models [Li et al., 2019], we can also set a reduction factor r (e.g., 2 or 4) to control the number of mel-spectrogram frames predicted at each decoding step, providing a balance between computational efficiency and the generation of high-quality speech. Formally, the original mel-spectrogram sequences \mathbf{y} will be partitioned into $\mathbf{y}^r = [\mathbf{y}_{0:r}, \mathbf{y}_{r:2r}, \dots, \mathbf{y}_{(T-r):T}]$ with reduction factor r , and the likelihood function can be expressed as follows:

$$p(\mathbf{y} | \mathbf{x}; \theta) = \prod_{t=0}^{T/r-1} p(\mathbf{y}_{t:r:(t+1)\cdot r} | \mathbf{y}_{<t:r}, \mathbf{x}; \theta) \quad (2)$$

During inference, MELLE executes zero-shot TTS tasks via prompting like VALL-E. Given the text content \mathbf{x} for synthesis, text transcription $\tilde{\mathbf{x}}$ and mel-spectrogram $\tilde{\mathbf{y}}$ of speech prompt, the model is designed to generate the target mel-spectrogram \mathbf{y} of the corresponding content while preserving the characteristics of the original speaker in prompt, with maximum likelihood probability as $\arg \max_{\mathbf{y}} p(\mathbf{y}_{t:r:(t+1)\cdot r} | [\tilde{\mathbf{x}}; \mathbf{x}; \tilde{\mathbf{y}}; \mathbf{y}_{<t:r}]; \theta)$ at each step, where $[\cdot]$ means concatenation operation and it backs to standard mode if $r = 1$.

3.2 MELLE Architecture

As illustrated in Figure 1, MELLE comprises the following main components: pre-nets that respectively convert text into sub-word tokens and extract mel-spectrograms from speech, before projecting them to the model dimension; an autoregressive (AR) Transformer decoder that serves as the language model; a latent sampling module that samples latent embedding from a predicted

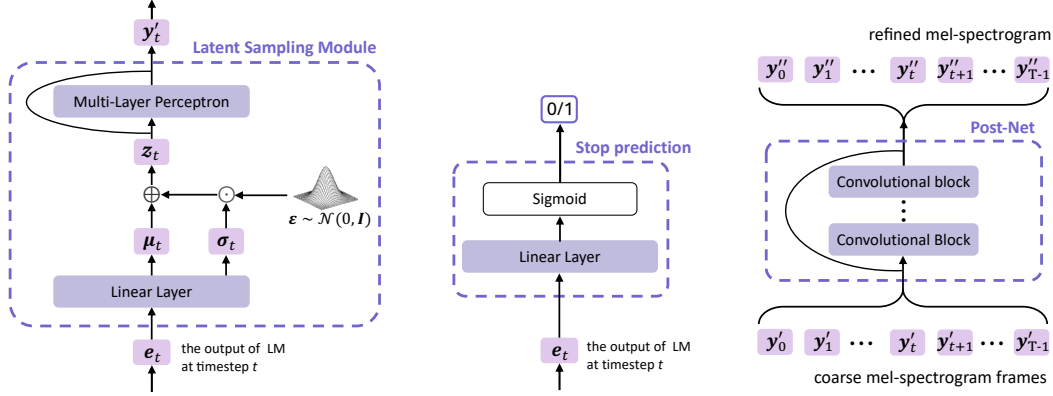


Figure 2: The Latent Sampling Module (left), Stop Prediction Layer (mid), and Post-Net (right).

Gaussian distribution, and then projects it back to the spectrogram space; a stop prediction layer that determines the end of the speech and a convolutional post-net for spectrogram refinement, similar to the methods described in [Shen et al., 2018, Li et al., 2019]. Finally, a vocoder is used to recover the speech from generated mel-spectrogram.

Unlike neural codec language models that iteratively predict multi-layer codec codes, we do not require an additional non-autoregressive (NAR) model thanks to the completeness of the mel-spectrogram. This simplification significantly improve computational and storage efficiency. Moreover, by adjusting the reduction factor, MELLE can generate multiple mel-spectrogram frames at one step, further enhancing efficiency while still maintaining superior performance.

3.2.1 Autoregressive Language Model

We employ a unidirectional Transformer decoder as the language model (LM) to autoregressively generates acoustic continuous features based on the textual input and acoustic prompts. Specifically, input text tokens x , with an appended $\langle \text{EOS} \rangle$ token, are first converted into embeddings by the text embedding layer based on their indices. Simultaneously, we employ a multi-layer perceptron, named pre-net, to project the mel-spectrogram y to the language model dimension. The LM, consisting of blocks of multi-head attention and feed-forward layers, takes the concatenation of text and acoustic embeddings as input to model the dependency between semantic and acoustic information. The output of the LM e_t at time step t is subsequently processed by the following modules of MELLE to synthesize the next-frame LM output, which is detailed in the following section.

3.2.2 Latent Sampling Module

Sampling strategy is an critical part in TTS systems, as it not only introduces diversity in the output, but also enhances the generalization ability of the model. For example, Tacotron-like models [Wang et al., 2017, Shen et al., 2018] enable dropout in their pre-net during inference to introduce variation; Neural codec language models [Wang et al., 2023, Zhang et al., 2023] adopt the top-p random sampling to avoid the collapse outputs leading by greedy search; Diffusion-based [Shen et al., 2024, Ju et al., 2024] and flow-matching-based methods [Le et al., 2024] restore speech representations from the sampling of a simpler distribution.

In this study, inspired by variational autoencoders (VAEs) [Kingma and Welling, 2014, Blei et al., 2017], we integrate a novel latent sampling module within MELLE, aimed at enhancing both expressive diversity and robustness, as shown in Figure 2 (left). Based on e_t , the output of the LM, this module predicts a distribution, from which a latent embedding z_t is sampled.

Specifically, we assume that z_t follows a multivariate Gaussian distribution where each dimension is independent. As depicted in Figure 2, a linear layer ($\mathbf{W}[\cdot] + \mathbf{b}$) predicts a mean vector μ_t and a log-magnitude variance vector $\log \sigma_t^2$ of the multivariate Gaussian distribution based on e_t . Leveraging

the reparameterization technique, a \mathbf{z}_t is sampled as

$$\mathbf{z}_t = \boldsymbol{\mu}_t + \boldsymbol{\sigma}_t \odot \boldsymbol{\epsilon} \quad (3)$$

$$\text{where } \boldsymbol{\epsilon} \sim \mathcal{N}(0, \mathbf{I}), \quad [\boldsymbol{\mu}_t, \log \boldsymbol{\sigma}_t^2] = \mathbf{W}e_t + \mathbf{b} \quad (4)$$

Therefore, the probability density function can be defined as

$$p_\theta(\mathbf{z}_t | e_t) = \mathcal{N}(\mathbf{z}_t | \boldsymbol{\mu}_t, \text{diag}(\boldsymbol{\sigma}_t^2)) \quad (5)$$

Note that the latent sampling module is differentiable with the reparameterization technique. Next, the latent variable \mathbf{z}_t is passed through a multi-layer perceptron (MLP) with residual connections, mapping it to the mel-spectrogram space as \mathbf{y}'_t , where $t = 0, 1, \dots, T - 1$.

3.2.3 Stop Prediction Layer and Post-Net

Since MELLE directly predicts continuous mel-spectrograms rather than discrete tokens, it cannot generate an <EOS> token to indicate the end of generation. Instead, we use a linear layer as a binary classifier, taking e_t to determine if the generation should conclude, as depicted in Figure 2 (mid). Following previous neural TTS models [Wang et al., 2017, Shen et al., 2018], we employ multiple convolutional blocks as the post-net to produce a residual that is added to $\mathbf{y}' = \{\mathbf{y}'_0, \mathbf{y}'_1, \dots, \mathbf{y}'_{T-1}\}$, resulting in the refined mel-spectrogram $\mathbf{y}'' = \{\mathbf{y}''_0, \mathbf{y}''_1, \dots, \mathbf{y}''_{T-1}\}$, as shown in Figure 2 (right). During training, the model is trained using teacher-forcing; while during inference, post-net processes \mathbf{y}' after the AR generation concludes.

3.3 Training Objective

The training process of MELLE is efficient and straightforward, due to the absence of VALL-E’s complex hierarchical structure. As illustrated in Figure 1, during training, a single end-to-end autoregressive model is optimized with the teacher-forcing manner using four loss functions: (1) a regression loss; (2) a Kullback-Leibler (KL) divergence loss; (3) a novel spectrogram flux loss; and (4) a binary cross entropy (BCE) loss for stop prediction. They work collaboratively to enhance overall performance:

$$\mathcal{L} = \mathcal{L}_{\text{reg}} + \lambda \mathcal{L}_{\text{KL}} + \beta \mathcal{L}_{\text{flux}} + \gamma \mathcal{L}_{\text{stop}} \quad (6)$$

Regression Loss The regression loss is a fundamental component of the training objective, ensuring the accurate prediction of mel-spectrogram frames, like conventional TTS [Li et al., 2019]. The regression loss, \mathcal{L}_{reg} , is composed of a combination of L1 and L2 losses, applied to both intermediate prediction \mathbf{y}' and final prediction \mathbf{y}'' of the mel-spectrogram. It is defined as follows:

$$\begin{aligned} \mathcal{L}_{\text{reg}}(\mathbf{y}, \mathbf{y}', \mathbf{y}'') &= \mathcal{L}_{\text{L1}}(\mathbf{y}, \mathbf{y}') + \mathcal{L}_{\text{L2}}(\mathbf{y}, \mathbf{y}') + \mathcal{L}_{\text{L1}}(\mathbf{y}, \mathbf{y}'') + \mathcal{L}_{\text{L2}}(\mathbf{y}, \mathbf{y}'') \\ &= \|\mathbf{y} - \mathbf{y}'\|_1 + \|\mathbf{y} - \mathbf{y}'\|_2^2 + \|\mathbf{y} - \mathbf{y}''\|_1 + \|\mathbf{y} - \mathbf{y}''\|_2^2 \end{aligned} \quad (7)$$

where \mathbf{y} represents the ground-truth mel-spectrogram target.

KL Divergence Loss We introduce a Kullback-Leibler (KL) divergence loss based on the concept of variational inference [Kingma and Welling, 2014, Blei et al., 2017], to enhance the diversity and stability of MELLE. The KL divergence measures the difference between the predicted latent distribution $p_\theta(\mathbf{z}_t | e_t)$ and a simpler distribution $p(\mathbf{z}_t)$. Unlike Kingma and Welling [2014], which selects $p(\mathbf{z}_t)$ as a standard normal distribution, we let \mathbf{z}_t possess the same dimensionality as the mel-spectrogram and define $p(\mathbf{z}_t)$ as $\mathcal{N}(\mathbf{y}_t, \mathbf{I})$. This can be seen as a shortcut on the optimization path thus accelerates the model’s learning. Combining equation (5), the KL divergence loss among T time steps can be analytically computed as

$$\begin{aligned} \mathcal{L}_{\text{KL}}(\mathbf{y}, \mathbf{z}) &= \sum_{t=0}^{T-1} D_{\text{KL}}(p_\theta(\mathbf{z}_t | e_t) \| p(\mathbf{z}_t)) \\ &= \frac{1}{2} \sum_{t=0}^{T-1} \sum_{i=1}^d (\boldsymbol{\sigma}_t^2[i] + (\boldsymbol{\mu}_t[i] - \mathbf{y}_t[i])^2 - 1 - \log \boldsymbol{\sigma}_t^2[i]) \end{aligned} \quad (8)$$

where d is the dimensionality of the feature space. The detailed derivation is provided in Appendix A.1. By integrating the KL divergence into the loss function, MELLE achieves a balance between reconstruction quality and latent space regularization, ultimately contributing to enhanced expressive diversity and robustness of the generated mel-spectrograms.

The Spectrogram Flux Loss To encourage the dynamic variation of the generated mel-spectrogram frames, we propose a novel spectrogram flux loss as a regularization term. This loss function penalizes low variability between consecutive frames, thereby promoting changes and preventing the generation of overly static mel-spectrograms:

$$\mathcal{L}_{\text{flux}}(\mathbf{y}, \boldsymbol{\mu}) = - \sum_{t=1}^{T-1} \|\boldsymbol{\mu}_t - \mathbf{y}_{t-1}\|_1 \quad (9)$$

where the L1 norm is employed to measure the difference between the predicted Gaussian mean vector $\boldsymbol{\mu}_t$ and the previous ground truth frame \mathbf{y}_{t-1} . By summing the negative value of the differences, the loss function rewards variations between frames, and the model is encouraged to reduce the generation of overly static frames that leading to repetition or endless silence in synthesized audio. Additionally, by penalizing flat predictions, the model is incentivized to produce more diverse and dynamic frame sequences, thereby preventing monotonic and unnatural speech.

Stop Prediction Loss We use a linear layer to project the output of the LM to a logit and calculate the BCE loss, $\mathcal{L}_{\text{stop}}$, for stop prediction, like TransformerTTS [Li et al., 2019] and SpeechT5 [Ao et al., 2022]. During this calculation, positive and negative frames are extremely imbalanced, as each utterance has only one positive frame indicating "stop." To address this, we impose a larger weight (100) for the positive frames in the BCE loss.

3.4 Inference: In-Context Learning for Mel-Spectrogram

During inference, we perform zero-shot text-to-speech by autoregressively predicting the mel-spectrogram. Given the text content x for synthesis, and a piece of speech prompt (with text transcription \tilde{x} and mel-spectrogram \tilde{y}), at each time step t , MELLE generates the next-frame mel-spectrogram y'_t from a latent embedding z_t , which is sampled from a distribution conditioned on the concatenation of \tilde{x} , x , \tilde{y} , and $y_{<t}$. After the AR generation process concludes, the coarse mel-spectrogram y' passes through the post-net to obtain the refined spectrogram y'' , which is then converted to speech audio using an off-the-shelf vocoder. If the reduction factor r is set, the input and predicted mel-spectrograms will be grouped by that factor.

In contrast to neural codec language models (e.g., VALL-E) that rely on multi-stage iterative predictions across multi-layer codec codes and require the manual configuration of sampling parameters, MELLE accomplishes speech synthesis in a single forward pass and automatically samples from learned distributions that are unique to each input. This automated approach ensures adaptive and consistent sampling, reduces human effort, and makes the method domain-independent. With the strong in-context learning capability from LLM, MELLE is capable of generating high-fidelity, natural-sounding speech for unseen speakers without fine-tuning.

4 Experimental Setup

4.1 Training Datasets

We trained MELLE on the Libriheavy [Kang et al., 2024] dataset, an annotated extension of the LibriLight [Kahn et al., 2020] corpus. Libriheavy contains approximately 50,000 hours of speech from 6,736 distinct speakers, sourced from open-source English audiobooks that are part of the LibriVox project. We use byte-pair encoding (BPE) [Sennrich et al., 2015] for text tokenization. For audios, we perform voice activity detection to remove abnormal silences and facilitate training. The 80-dimensional log-magnitude mel-spectrograms are extracted from waveforms resampled at 16 kHz. The detailed extraction protocol of mel-spectrogram can be found in Appendix A.2.

To facilitate comparison with research conducted with constrained resources [Song et al., 2024, Han et al., 2024], we also trained a constrained version of MELLE on LibriSpeech [Panayotov et al., 2015], which contains 960 hours of data from 1,251 speakers. We use phoneme text tokens for this version. This limited version, denoted as MELLE-*limited* in the subsequent sections, aims to verify the effectiveness of our model when trained on relatively small datasets.

4.2 Experimental Setting

Model Configurations Following VALL-E, the language model of MELLE incorporates 12 Transformer blocks, each with 16 attention heads, an embedding dimension of 1,024, a feed-forward layer dimension of 4,096, and a dropout rate set at 0.1. The input mel-spectrograms are projected to the model’s embedding dimensionality using a 3-layer perceptron with a 0.5 dropout rate enabled during both training and inference, following Wang et al. [2017]. Within the latent sampling module, a linear layer is used to derive the mean vector μ_t and the log-variance vector $\log \sigma_t^2$ of the latent distribution. The sampled z_t passes through a 3-layer perceptron to produce a residual, which is then added to itself to generate y'_t . The post-net, consisting of 5 convolutional blocks with a kernel size of 5 and 256 intermediate channels, takes y' to generate the refined mel-spectrogram y'' . Throughout this study, we utilize the open-source HiFi-GAN vocoder² [Kong et al., 2020], trained on 585-hour LibriTTS corpus, to recover audio from mel-spectrogram.

Training Details MELLE models are trained on 16 NVIDIA Tesla V100 32GB GPUs with a total batch size of 480K input frames for 400K update steps. While MELLE-*limited* is trained on 8 GPUs with a total batch size of about 80K input frames for 400K steps. We optimize the models using the AdamW optimizer, warming up the learning rate to a peak of 5×10^{-4} over the first 32K updates, followed by a linear decay. We set $\beta = 0.5$ and $\gamma = 1.0$ for the spectrogram flux loss and the stop prediction loss term. For the KL divergence loss, we set $\lambda = 0$ for the first 10K steps to ensure stable training, and $\lambda = 0.1$ thereafter.

4.3 Evaluation Settings

We use LibriSpeech test-clean set for zero-shot test-to-speech evaluation, ensuring that none of the speakers from this corpus are included in the training data. Following recent works [Wang et al., 2023, Chen et al., 2024], we screen audios with the length ranging from 4 to 10 seconds for evaluation. We measure the performance of MELLE under two inference schemes: (1) *Continuation*: We use the text transcription and the first 3 seconds of the utterance as the prompt, expecting the model to seamlessly synthesize the subsequent portion of the speech; (2) *Cross-sentence*: Using a reference utterance and its transcription from the same speaker as the prompt, and given the text of the target utterance, we expect the model to synthesize the corresponding speech while retaining the characteristics of the reference speaker.

To assess the naturalness, robustness, speaker similarity and efficiency of the proposed method, we employ multiple subjective and objective metrics:

WER (word error rate) Previous codec language models often face robustness issues, including word deletion, insertion, replacement, and predicting endless silence or noise. To assess robustness and intelligibility, we perform speech recognition on the synthesized speech using both a Conformer-Transducer model³ [Gulati et al., 2020] and HuBERT-Large ASR model⁴ [Hsu et al., 2021]. We then calculate WER between the transcripts and the ground truth text to compare MELLE against other systems. We use WER-C and WER-H to denote the WER obtained from the two ASR systems.

SIM (speaker similarity) Speaker similarity reflects the in-context learning capability of zero-shot TTS models. We utilize WavLM-TDNN⁵ [Chen et al., 2022] to extract speaker embedding vectors from the reference speech prompt and the generated speech. The cosine distance between them is then calculated to measure speaker similarity, with the range of [-1, 1]. We compute SIM-r and SIM-o, where SIM-r measures the similarity between the synthesized speech and the speech prompt reconstructed from the mel-spectrogram with the vocoder, whereas SIM-o measures the similarity with respect to the original speech prompt. Considering that SIM-r is not comparable among systems using different acoustic tokens, we recommend referring to SIM-o.

Subjective metrics We engaged native English speakers with experience in speech annotation and evaluation to participate as contributors in a crowd-sourced evaluation. Each utterance was assessed

²The pre-trained vocoder can be found in <https://huggingface.co/mechanicalsea/speecht5-tts>

³https://huggingface.co/nvidia/stt_en_conformer_transducer_xlarge

⁴<https://huggingface.co/facebook/hubert-large-ls960-ft>

⁵https://github.com/microsoft/UniSpeech/tree/main/downstreams/speaker_verification

by at least 10 native speakers from various perspectives. The crowd-sourcing platform also oversaw and validated the testing process and results. The evaluation uses three types of mean opinion scores (MOS): (1) MOS for assessing speech quality; (2) Similarity MOS (SMOS) for measuring speaker similarity between the speech prompt and the generated speech; and (3) Comparative MOS (CMOS) for evaluating the comparative naturalness of the synthesized speech against the original ground truth audio. For the MOS and SMOS evaluations, each test sample is rated on a scale from 1 to 5, in 0.5-point increments. Higher scores indicate more positive evaluations. For the CMOS evaluation, the ground-truth sample and the generated sample are presented in random order to participants, who assign scores from -3 (much worse than the baseline) to 3 (much better than the baseline), with intervals of 1. We evaluate 40 samples from our test set, with one sample per speaker.

Inference time MELLE supports adjusting the reduction factor r to predict multiple mel-spectrogram frames at each time step, thereby shortening the sequence length and accelerating both model training and inference. We evaluate the efficiency of MELLE with different reduction factors in our experiments by measuring the inference time for generating 10-second speech segments, averaged over ten trials, and compared it with other systems.

5 Results and Discussion

In this section, we compare the speech synthesis performance of MELLE with various systems⁶, and conduct the discussion about inference efficiency and ablation study. Particularly, we would like to point out that, as shown in Table 1, the ground-truth speech reconstructed from mel-spectrograms demonstrates higher robustness and speaker similarity, compared to speech reconstructed from EnCodec codes. This confirms our hypothesis that discrete codec codes, originally designed for audio compression, sacrifice fidelity compared to the well-established continuous mel-spectrogram.

5.1 Objective Evaluation

As illustrated in Table 1, the proposed MELLE outperforms VALL-E and all its variants on the *continuation* zero-shot speech synthesis task, and it is comparable to VALL-E 2 on the *cross-sentence* task. Most importantly, it presents a much more concise and efficient paradigm for audio language modeling without vector quantization.

Compared to vanilla VALL-E, MELLE significantly outperforms it in terms of both robustness and speaker similarity, achieving a 47.9% relative reduction in WER-H on the continuation task and a 64.4% reduction on the cross-sentence task. Studies such as ELLA-V and VALL-E R, which explicitly introduce some monotonic alignment mechanism into the language model, have helped improve robustness to some extent, as reflected in the WER metric. However, it comes at the cost of a significant decrease in speaker similarity as shown in Table 1. CLaM-TTS demonstrated acceptable performance on continuation tasks, but its performance is limited on cross-sentence tasks. It introduces more complex assumptions and therefore a more intricate structure. Despite both being single-stage models, the MELLE outperforms it by a large margin featuring a simpler topology. VALL-E 2 proposes a repetition-aware sampling method and employs Vocos [Siuzdak, 2024] as its audio codec decoder, demonstrating results on par with ours. For the continuation task, MELLE reveals better robustness and speaker similarity. This indicates that MELLE exhibits superior zero-shot capabilities with even shorter prompts, highlighting its in-context learning ability. We attribute this advantage to our direct prediction of the mel-spectrogram, which encompasses richer acoustic cues compared to abstract discrete codes. For the cross-sentence task, although MELLE falls slightly behind in the objective speaker similarity metric, it still significantly surpasses VALL-E 2 in subjective evaluation metrics, as evidenced in Table 3. We attribute the slight difference in this objective metric to speaker verification model bias, considering that MELLE achieves a higher SIM-o compared to VALL-E 2 (0.680 vs. 0.662), when evaluated using another well-recognized speaker verification model, ECAPA-TDNN.

Although Voicebox demonstrates better speaker similarity than MELLE, we argue that this gap can be partially attributed to their proprietary vocoder, which was trained on a 60,000-hour corpus. In contrast, MELLE utilizes an open-source vocoder trained on the 585-hour LibriTTS corpus.

⁶We do not include the results of NaturalSpeech 3 reported in Ju et al. [2024] in our comparisons, as it uses a 40-utterance test set which is different with other studies.

Table 1: Objective performance comparison on *continuation* and *cross-sentence* zero-shot speech synthesis tasks. WER-C (%) denotes evaluation with the Conformer-Transducer ASR model, while WER-H (%) denotes evaluation with the HuBERT-Large ASR model. MELLE- R_x denotes the model is with a reduction factor of x . MELLE-*limited* denotes the model is trained on small-scale corpus. The **boldface** indicates the best result, and the underline denotes the second best. *We quote Han et al. [2024]’s reproduction results, which demonstrate better performance. †We evaluate metrics not reported in the original paper, using the audios provided by the authors.

| System | Continuation | | | | Cross-Sentence | | | |
|--------------------------------|--------------|-------------|--------------|--------------|----------------|-------------|--------------|--------------|
| | WER-C | WER-H | SIM-r | SIM-o | WER-C | WER-H | SIM-r | SIM-o |
| Ground Truth | 1.61 | 2.15 | - | 0.668 | 1.61 | 2.15 | - | 0.779 |
| Ground Truth (codec) | 1.65 | 2.33 | 0.604 | 0.593 | 1.65 | 2.33 | 0.738 | 0.710 |
| Ground Truth (mel) | 1.64 | 2.24 | 0.622 | 0.617 | 1.64 | 2.24 | 0.747 | 0.732 |
| ELLA-V [Song et al., 2024] * | 2.10 | 2.91 | 0.340 | 0.303 | 7.15 | 8.90 | 0.331 | 0.307 |
| VALL-E R [Han et al., 2024] † | 1.58 | 2.32 | 0.397 | 0.363 | 3.18 | 3.97 | 0.395 | 0.365 |
| RALL-E [Xin et al., 2024] | - | - | - | - | 2.5 | 2.8 | - | 0.49 |
| CLaM-TTS [Kim et al., 2024] | - | 2.36 | 0.513 | 0.477 | - | 5.11 | 0.538 | 0.495 |
| VALL-E [Wang et al., 2023] | - | 3.8 | 0.508 | - | - | 5.9 | 0.580 | - |
| VALL-E 2 [Chen et al., 2024] † | 1.6 | 2.32 | 0.529 | 0.504 | <u>1.5</u> | 2.44 | <u>0.678</u> | <u>0.643</u> |
| Voicebox [Le et al., 2024] | - | <u>2.0</u> | 0.616 | 0.593 | - | 1.9 | 0.681 | 0.662 |
| MELLE | <u>1.47</u> | 1.98 | <u>0.539</u> | <u>0.508</u> | 1.47 | <u>2.10</u> | 0.664 | 0.625 |
| MELLE-R2 | 1.45 | 2.02 | 0.522 | 0.489 | <u>1.50</u> | 2.14 | 0.651 | 0.608 |
| MELLE-R3 | 1.52 | 2.10 | 0.502 | 0.462 | 1.51 | 2.19 | 0.620 | 0.570 |
| MELLE-R4 | 1.59 | 2.10 | 0.480 | 0.437 | 1.56 | 2.30 | 0.589 | 0.532 |
| MELLE-R5 | 1.66 | 2.25 | 0.455 | 0.410 | 1.96 | 2.72 | 0.564 | 0.506 |
| MELLE- <i>limited</i> | 1.53 | 2.22 | 0.517 | 0.480 | 2.21 | 2.80 | 0.633 | 0.591 |

Table 2: Comparison of five-time sampling performance with different reduction factors on *continuation* and *cross-sentence* zero-shot speech synthesis tasks. The five-time sampling results indicate the upper bound of the systems’ performance.

| System | Continuation | | | | Cross-Sentence | | | |
|-----------------------|--------------|-------------|--------------|--------------|----------------|-------------|--------------|--------------|
| | WER-C | WER-H | SIM-r | SIM-o | WER-C | WER-H | SIM-r | SIM-o |
| Ground Truth | 1.61 | 2.15 | - | 0.668 | 1.61 | 2.15 | - | 0.779 |
| MELLE | 1.03 | 1.49 | 0.590 | 0.561 | 0.70 | 1.07 | 0.700 | 0.663 |
| MELLE-R2 | 1.04 | 1.47 | 0.575 | 0.542 | 0.77 | 1.12 | 0.688 | 0.647 |
| MELLE-R3 | 1.12 | 1.54 | 0.550 | 0.512 | 0.86 | 1.17 | 0.656 | 0.608 |
| MELLE-R4 | 1.11 | 1.52 | 0.527 | 0.487 | 0.76 | 1.08 | 0.625 | 0.571 |
| MELLE-R5 | 1.05 | 1.52 | 0.507 | 0.463 | 0.93 | 1.38 | 0.603 | 0.547 |
| MELLE- <i>limited</i> | 1.04 | 1.57 | 0.566 | 0.533 | 1.04 | 1.50 | 0.672 | 0.631 |

Additionally, Voicebox requires both phoneme and duration information for speech synthesis. In contrast, MELLE just requires BPE text as input which is user-friendly.

Referring to previous work on predicting mel-spectrograms, MELLE can accelerate training and inference by predicting multiple frames through an adjustable reduction factor r . We observe that as the reduction factor increases, the robustness remains consistently at a high level for both the continuation and cross-sentence tasks. Although speaker similarity declines due to the prediction of multiple consecutive frames at once, MELLE still remarkably outperforms most recent works in both robustness and speaker similarity, even with a large reduction factor r , as shown in Table 1. MELLE-*limited*, which is trained on the relatively small-scale LibriSpeech corpus, also demonstrates superior performance compared to VALL-E and its variants, apart from VALL-E 2.

A potential use of MELLE is to set a larger reduction factor r while sampling multiple times, selecting the candidate with the highest speaker similarity to the prompt as the final output. This strategy can enhance performance while reducing inference time, as the process can be executed in parallel on the GPU. To explore the upper bound performance of MELLE with different r , we report five-time sampling results in Table 2. In this setup, we sample five times for each test utterance and select the candidate with the best score for each metric. MELLE models consistently demonstrate high robustness across different r settings, achieving much lower WER than the ground truth.

Table 3: Subjective evaluation results for 40 speakers from the LibriSpeech test-clean dataset. We use a reference utterance as the prompt for each speaker.

| System | MOS | SMOS | CMOS |
|---------------------------------|------------------------|------------------------|---------------|
| Ground Truth | 4.29 \pm 0.16 | 3.94 \pm 0.25 | 0.000 |
| YourTTS [Casanova et al., 2022] | 2.41 \pm 0.24 | 2.62 \pm 0.25 | -2.162 |
| VALL-E [Wang et al., 2023] | 3.18 \pm 0.23 | 3.50 \pm 0.25 | -0.912 |
| VALL-E 2 [Chen et al., 2024] | 4.08 \pm 0.18 | 3.88 \pm 0.25 | -0.085 |
| MELLE | 4.20 \pm 0.20 | 4.40 \pm 0.22 | -0.032 |
| MELLE-R2 | 4.14 \pm 0.19 | 4.18 \pm 0.24 | -0.252 |

Table 4: Ablation study on the effectiveness of latent sampling and the spectrogram flux loss. The \blacklozenge denotes that latent sampling is enabled during training but disabled during inference.

| | Latent Sampling | Spectrogram Flux Loss | Continuation | | | | Cross-Sentence | | | |
|----------------------|-----------------|-----------------------|--------------|-------------|--------------|--------------|----------------|-------------|--------------|--------------|
| | | | WER-C | WER-H | SIM-r | SIM-o | WER-C | WER-H | SIM-r | SIM-o |
| Single-Time Sampling | \times | \times | 6.41 | 6.91 | 0.511 | 0.483 | 23.21 | 23.65 | 0.550 | 0.518 |
| | \checkmark | \times | 3.57 | 4.07 | 0.521 | 0.486 | 10.36 | 10.87 | 0.629 | 0.584 |
| | \times | \checkmark | 2.03 | 2.61 | 0.529 | 0.506 | 5.31 | 5.90 | 0.631 | 0.602 |
| | \blacklozenge | \checkmark | 1.54 | 2.13 | 0.533 | 0.506 | 2.10 | 2.72 | 0.649 | 0.615 |
| | \checkmark | \checkmark | 1.47 | 1.98 | 0.539 | 0.508 | 1.47 | 2.10 | 0.664 | 0.625 |
| Five-Time Sampling | \times | \times | 3.74 | 4.15 | 0.562 | 0.536 | 17.69 | 18.00 | 0.601 | 0.569 |
| | \checkmark | \times | 1.18 | 1.63 | 0.580 | 0.546 | 2.41 | 2.86 | 0.686 | 0.641 |
| | \times | \checkmark | 1.17 | 1.65 | 0.573 | 0.551 | 1.74 | 2.13 | 0.672 | 0.644 |
| | \blacklozenge | \checkmark | 1.10 | 1.50 | 0.579 | 0.552 | 1.07 | 1.47 | 0.678 | 0.645 |
| | \checkmark | \checkmark | 1.03 | 1.49 | 0.590 | 0.561 | 0.70 | 1.07 | 0.700 | 0.663 |

5.2 Subjective Evaluation

We conduct subjective evaluations using a crowd-source human rating system to assess MOS, SMOS, and CMOS, which correspond to overall speech quality, speaker similarity, and naturalness of the synthesized speech, respectively. For each speaker, we use their preceding utterance from the official LibriSpeech test set list as the prompt to generate the target utterance, resulting in 40 test cases. We use the original 16 kHz audios as the ground truth in the evaluations, unlike VALL-E 2 paper which utilizes 24 kHz upsampled audios as the ground truth.

As shown in Table 3, MELLE’s synthesized speech is more favorably received by human listeners, achieving the best performance across all metrics compared to VALL-E 2, VALL-E, and YourTTS. Remarkably, MELLE attains a higher SMOS score than even the ground truth (4.40 vs. 3.94), highlighting its exceptional capability to capture and retain the speaker’s characteristics. Furthermore, MELLE achieves comparable performance in terms of speech quality (CMOS: -0.032 for ours vs. ground truth, with p -value > 0.1 according to a t-test), indicating that our model can generate accurate and natural speech, on par with human performance. Besides, MELLE-R2, despite sacrificing some performance for efficiency, still outperforms VALL-E 2 in both MOS and SMOS.

We found that MELLE’s latent sampling, which avoids manually designed sampling strategies for discrete codec codes, enables it to generate more stable and natural speech compared to both VALL-E 2 and VALL-E. We recommend visiting our demo website for more information.

5.3 Ablation Study

To assess the effectiveness of the proposed methods, we conduct a series of ablation studies on MELLE, reporting both single-time and five-time sampling results. If the latent sampling is marked as disabled in Table 4, it will degrade into a simple linear layer without reparameterization.

From the results presented in Table 4, both the proposed latent sampling method and the spectrogram flux loss significantly enhance the robustness (reflected by WER) and speaker similarity of the synthesized speech. This improvement is particularly pronounced in the cross-sentence inference task, suggesting that the proposed methods substantially facilitate long sequence modeling. We also

Table 5: Inference time (in seconds) for generating a 10-second speech segment. "AR" represents "autoregressive". The "105" refers to the number of auxiliary tokens need to predict, corresponding to the number of textual tokens, totaling approximately 105 according to statistics. *Results quoted from Han et al. [2024]. †Results quoted from Kim et al. [2024]; Voicebox is with 64 NFE.

| System | Average AR Steps | Average Inference Time |
|-------------------------------|----------------------|------------------------|
| VALL-E [Wang et al., 2023] * | 750 | 10.27 |
| ELLA-V [Song et al., 2024] * | $\sim 105 * 2 + 750$ | 15.76 |
| RALL-E [Xin et al., 2024] * | $\sim 105 + 750$ | 12.28 |
| VALL-E R [Han et al., 2024] * | 375 | 3.67 |
| VoiceBox [Le et al., 2024] † | - | 6.4 |
| CLaM-TTS [Kim et al., 2024] † | - | 4.15 |
| VALL-E [Wang et al., 2023] | 750 | 7.32 |
| VALL-E 2 [Chen et al., 2024] | 750 | 7.32 |
| MELLE | ~ 620 | 5.49 |
| MELLE-R2 | ~ 310 | 2.76 |
| MELLE-R4 | ~ 155 | 1.40 |

conduct an experiment where latent sampling is enabled during training but disabled during inference. The results indicate that the latent sampling during inference leads to more robust and natural outputs.

We would like to emphasize the role of the latent sampling method in improving speaker similarity. Compared to the spectrogram flux loss, latent sampling offers relatively less improvement in WER, yet it provides comparable gains in speaker similarity. This indicates that the primary function of latent sampling is to capture and preserve the speaker characteristics present in the speech prompt. On the other hand, the spectrogram flux loss improves SIM-r and SIM-o partly by enhancing the model’s robustness and ensuring the accurate generation of semantic context.

5.4 Efficiency Comparison

In this section, we compare the inference time for generating 10-second speech segments across different acoustic language models. Since VALL-E and VALL-E 2 (without code grouping) share the identical architecture but differ in sampling strategies, their inference time can be considered the same. As shown in Table 5, MELLE is more efficient than VALL-E, as it forgoes the non-autoregressive (NAR) inference steps, thereby reducing both computational and spatial complexity. Moreover, the mel-spectrograms are extracted at approximately 62 Hz, whereas the EnCodec codes used by VALL-E is at 75 Hz.

ELLA-V predicts acoustic tokens alongside phonemes to introduce a monotonic alignment mechanism, while RALL-E predicts duration and pitch tokens for each phoneme before generating the acoustic tokens. Both approaches incorporate additional supervision and conditions to drive robust outputs, but also introduce considerable overhead in both inference and training.

By setting the reduction factor r , the training and inference processes of MELLE can be accelerated by approximately r times. As shown in Table 5, MELLE-R2 halves the inference time, while MELLE-R4 reduces it to one quarter, surpassing both CLaM-TTS and Voicebox. Despite the reductions, they still demonstrate satisfactory performance, as revealed in Table 1 and Table 2.

6 Conclusion

In this study, we propose a continuous acoustic representation-based language modeling approach for zero-shot text-to-speech synthesis tasks, thereby eliminating the use of discrete vector quantization. By exploring the potential of mel-spectrograms within the paradigm of language modeling, the proposed MELLE directly predicts mel-spectrograms conditioned on text content and speech prompt. This approach eliminates the need for the two-pass training and inference procedures typical of neural codec language model VALL-E, and can further accelerate decoding by setting the reduction factor. With the aid of latent sampling and spectrogram flux loss, MELLE is capable of producing more

diverse and robust predictions, attaining results comparable to human performance in subjective evaluations.

7 Limitations and Broader Impact

Limitations Despite MELLE’s promising performance and concise topology, we acknowledge several limitations. First, the quality of the synthesized speech can be limited by the capabilities of the vocoder utilized. We anticipate performance improvements by training a more powerful vocoder on a large-scale corpus, as demonstrated by Voicebox [Le et al., 2024]. Second, our work conduct evaluation on English-only LibriSpeech test set. Multi-lingual setting like VALL-E X [Zhang et al., 2023] on various dataset will be explored in our future work. Third, we adopt the mel-spectrogram as the target continuous acoustic representation throughout this work. Future research will explore other continuous representations, such as VAE latent hidden states.

Broader Impact We envision advancing the development of audio and speech synthesis models by distilling the methodology of audio language modeling to its fundamental principles, eliminating the complexity of heavy codebooks. The proposed approach can substantially reduce the training and inference costs of large-scale audio generation models while improving performance.

MELLE is purely a research project. Currently, we have no plans to incorporate MELLE into a product or expand access to the public. MELLE could synthesize speech that maintains speaker identity and could be used for education, entertainment, journalistic, self-authored content, accessibility features, interactive voice response systems, translation, chat-bot, and so on. While MELLE can speak in a voice like the voice talent, the similarity, and naturalness depend on the length and quality of the speech prompt, the background noise, as well as other factors. It may carry potential risks in the misuse of the model, such as spoofing voice identification or impersonating a specific speaker. We conducted the experiments under the assumption that the user agrees to be the target speaker in speech synthesis. If the model is generalized to unseen speakers in the real world, it should include a protocol to ensure that the speaker approves the use of their voice and a synthesized speech detection model. If you suspect that MELLE is being used in a manner that is abusive or illegal or infringes on your rights or the rights of other people, you can report it at the Report Abuse Portal.

References

- Philip Anastassiou, Jiawei Chen, Jitong Chen, Yuanzhe Chen, Zhuo Chen, Ziyi Chen, Jian Cong, Lelai Deng, Chuang Ding, Lu Gao, et al. Seed-TTS: A family of high-quality versatile speech generation models. *arXiv preprint arXiv:2406.02430*, 2024.
- Junyi Ao, Rui Wang, Long Zhou, Chengyi Wang, Shuo Ren, Yu Wu, Shujie Liu, Tom Ko, Qing Li, Yu Zhang, Zhihua Wei, Yao Qian, Jinyu Li, and Furu Wei. SpeechT5: Unified-modal encoder-decoder pre-training for spoken language processing. In *Proceedings of the 60th Annual Meeting of the Association for Computational Linguistics*, pages 5723–5738, 2022.
- Alan W Black and Paul A Taylor. Automatically clustering similar units for unit selection in speech synthesis. 1997.
- David M. Blei, Alp Kucukelbir, and Jon D. McAuliffe. Variational inference: A review for statisticians. *Journal of the American Statistical Association*, 112(518):859–877, 2017.
- Zalán Borsos, Raphaël Marinier, Damien Vincent, Eugene Kharitonov, Olivier Pietquin, Matt Sharifi, Olivier Teboul, David Grangier, Marco Tagliasacchi, and Neil Zeghidour. AudioLM: a language modeling approach to audio generation. *arXiv preprint arXiv:2209.03143*, 2022.
- Zalán Borsos, Matt Sharifi, Damien Vincent, Eugene Kharitonov, Neil Zeghidour, and Marco Tagliasacchi. SoundStorm: Efficient parallel audio generation. *arXiv preprint arXiv:2305.09636*, 2023.
- Tom Brown, Benjamin Mann, Nick Ryder, Melanie Subbiah, Jared D Kaplan, Prafulla Dhariwal, Arvind Neelakantan, Pranav Shyam, Girish Sastry, Amanda Askell, et al. Language models are few-shot learners. *Advances in neural information processing systems*, 33:1877–1901, 2020.

- Edresson Casanova, Julian Weber, Christopher D Shulby, Arnaldo Candido Junior, Eren Gölge, and Moacir A Ponti. YourTTS: Towards zero-shot multi-speaker TTS and zero-shot voice conversion for everyone. In *International Conference on Machine Learning*, pages 2709–2720, 2022.
- Sanyuan Chen, Chengyi Wang, Zhengyang Chen, Yu Wu, Shujie Liu, Zhuo Chen, Jinyu Li, Naoyuki Kanda, Takuya Yoshioka, Xiong Xiao, et al. WavLM: Large-scale self-supervised pre-training for full stack speech processing. *IEEE Journal of Selected Topics in Signal Processing*, 16(6): 1505–1518, 2022.
- Sanyuan Chen, Shujie Liu, Long Zhou, Yanqing Liu, Xu Tan, Jinyu Li, Sheng Zhao, Yao Qian, and Furu Wei. VALL-E 2: Neural codec language models are human parity zero-shot text to speech synthesizers. *arXiv preprint arXiv:2406.05370*, 2024.
- Alexandre Défossez, Jade Copet, Gabriel Synnaeve, and Yossi Adi. High fidelity neural audio compression. *Transactions on Machine Learning Research*, 2023. Featured Certification, Reproducibility Certification.
- Sefik Emre Eskimez, Xiaofei Wang, Manthan Thakker, Canrun Li, Chung-Hsien Tsai, Zhen Xiao, Hemin Yang, Zirun Zhu, Min Tang, Xu Tan, et al. E2 TTS: Embarrassingly easy fully non-autoregressive zero-shot TTS. *arXiv preprint arXiv:2406.18009*, 2024.
- Anmol Gulati, James Qin, Chung-Cheng Chiu, Niki Parmar, Yu Zhang, Jiahui Yu, Wei Han, Shibo Wang, Zhengdong Zhang, Yonghui Wu, and Ruoming Pang. Conformer: Convolution-augmented transformer for speech recognition. In *Proc. Interspeech 2020*, pages 5036–5040, 2020.
- Bing Han, Long Zhou, Shujie Liu, Sanyuan Chen, Lingwei Meng, Yanming Qian, Yanqing Liu, Sheng Zhao, Jinyu Li, and Furu Wei. VALL-E R: Robust and efficient zero-shot text-to-speech synthesis via monotonic alignment. *arXiv preprint arXiv:2406.07855*, 2024.
- Wei-Ning Hsu, Benjamin Bolte, Yao-Hung Hubert Tsai, Kushal Lakhota, Ruslan Salakhutdinov, and Abdelrahman Mohamed. HuBERT: Self-supervised speech representation learning by masked prediction of hidden units. *IEEE/ACM Trans. Audio, Speech and Lang. Proc.*, 29:3451–3460, 2021.
- Mengqi Huang, Zhendong Mao, Quan Wang, and Yongdong Zhang. Not all image regions matter: Masked vector quantization for autoregressive image generation. In *Proceedings of the IEEE/CVF Conference on Computer Vision and Pattern Recognition*, pages 2002–2011, 2023.
- Andrew J Hunt and Alan W Black. Unit selection in a concatenative speech synthesis system using a large speech database. In *1996 IEEE international conference on acoustics, speech, and signal processing conference proceedings*, volume 1, pages 373–376, 1996.
- Keith Ito and Linda Johnson. The LJ speech dataset. <https://keithito.com/LJ-Speech-Dataset/>, 2017.
- Ziyue Jiang, Yi Ren, Zhenhui Ye, Jinglin Liu, Chen Zhang, Qian Yang, Shengpeng Ji, Rongjie Huang, Chunfeng Wang, Xiang Yin, et al. Mega-TTS: Zero-shot text-to-speech at scale with intrinsic inductive bias. *arXiv preprint arXiv:2306.03509*, 2023.
- Zeqian Ju, Yuancheng Wang, Kai Shen, Xu Tan, Detai Xin, Dongchao Yang, Yanqing Liu, Yichong Leng, Kaitao Song, Siliang Tang, et al. Naturalspeech 3: Zero-shot speech synthesis with factorized codec and diffusion models. *arXiv preprint arXiv:2403.03100*, 2024.
- Jacob Kahn, Morgane Rivière, Weiyi Zheng, Evgeny Kharitonov, Qiantong Xu, Pierre-Emmanuel Mazaré, Julien Karadayi, Vitaliy Liptchinsky, Ronan Collobert, Christian Fuegen, et al. Libri-light: A benchmark for asr with limited or no supervision. In *ICASSP*, pages 7669–7673, 2020.
- Wei Kang, Xiaoyu Yang, Zengwei Yao, Fangjun Kuang, Yifan Yang, Liyong Guo, Long Lin, and Daniel Povey. Libriheavy: a 50,000 hours asr corpus with punctuation casing and context. In *ICASSP 2024-2024 IEEE International Conference on Acoustics, Speech and Signal Processing (ICASSP)*, pages 10991–10995, 2024.

- Jaehyeon Kim, Keon Lee, Seungjun Chung, and Jaewoong Cho. CLaM-TTS: Improving neural codec language model for zero-shot text-to-speech. In *The Twelfth International Conference on Learning Representations*, 2024.
- Diederik P Kingma and Max Welling. Auto-encoding variational bayes. In *The International Conference on Learning Representations*, 2014.
- Jungil Kong, Jaehyeon Kim, and Jaekyoung Bae. HiFi-GAN: Generative adversarial networks for efficient and high fidelity speech synthesis. In *Advances in Neural Information Processing Systems*, volume 33, pages 17022–17033, 2020.
- Mateusz Łajszczak, Guillermo Cámbara, Yang Li, Fatih Beyhan, Arent van Korlaar, Fan Yang, Arnaud Joly, Álvaro Martín-Cortinas, Ammar Abbas, Adam Michalski, et al. BASE TTS: Lessons from building a billion-parameter text-to-speech model on 100K hours of data. *arXiv preprint arXiv:2402.08093*, 2024.
- Matthew Le, Apoorv Vyas, Bowen Shi, Brian Karrer, Leda Sari, Rashel Moritz, Mary Williamson, Vimal Manohar, Yossi Adi, Jay Mahadeokar, et al. Voicebox: Text-guided multilingual universal speech generation at scale. *Advances in neural information processing systems*, 36, 2024.
- Naihan Li, Shujie Liu, Yanqing Liu, Sheng Zhao, and Ming Liu. Neural speech synthesis with transformer network. *Proceedings of the AAAI Conference on Artificial Intelligence*, page 6706–6713, Aug 2019.
- Tianhong Li, Yonglong Tian, He Li, Mingyang Deng, and Kaiming He. Autoregressive image generation without vector quantization. *arXiv preprint arXiv:2406.11838*, 2024a.
- Yinghao Aaron Li, Cong Han, Vinay Raghavan, Gavin Mischler, and Nima Mesgarani. StyleTTS 2: Towards human-level text-to-speech through style diffusion and adversarial training with large speech language models. *Advances in Neural Information Processing Systems*, 36, 2024b.
- Aaron van den Oord, Sander Dieleman, Heiga Zen, Karen Simonyan, Oriol Vinyals, Alex Graves, Nal Kalchbrenner, Andrew Senior, and Koray Kavukcuoglu. WaveNet: A generative model for raw audio. *arXiv preprint arXiv:1609.03499*, 2016.
- OpenAI et al. GPT-4 technical report. *arXiv preprint arXiv:2303.08774*, 2023.
- Vassil Panayotov, Guoguo Chen, Daniel Povey, and Sanjeev Khudanpur. Librispeech: An ASR corpus based on public domain audio books. In *ICASSP*, pages 5206–5210, 2015.
- Krishna C. Puvvada, Nithin Rao Koluguri, Kunal Dhawan, Jagadeesh Balam, and Boris Ginsburg. Discrete audio representation as an alternative to mel-spectrograms for speaker and speech recognition. In *ICASSP 2024 - 2024 IEEE International Conference on Acoustics, Speech and Signal Processing (ICASSP)*, pages 12111–12115, 2024.
- Yi Ren, Yangjun Ruan, Xu Tan, Tao Qin, Sheng Zhao, Zhou Zhao, and Tie-Yan Liu. FastSpeech: Fast, robust and controllable text to speech. In *NeurIPS*, pages 3165–3174, 2019.
- Robin Rombach, Andreas Blattmann, Dominik Lorenz, Patrick Esser, and Björn Ommer. High-resolution image synthesis with latent diffusion models. In *Proceedings of the IEEE/CVF conference on computer vision and pattern recognition*, pages 10684–10695, 2022.
- Rico Sennrich, Barry Haddow, and Alexandra Birch. Neural machine translation of rare words with subword units. *arXiv preprint arXiv:1508.07909*, 2015.
- Jonathan Shen, Ruoming Pang, Ron J. Weiss, Mike Schuster, Navdeep Jaitly, Zongheng Yang, Zhifeng Chen, Yu Zhang, Yuxuan Wang, RJ-Skerrv Ryan, Rif A. Saurous, Yannis Agiomyrgiannakis, and Yonghui Wu. Natural TTS synthesis by conditioning wavenet on MEL spectrogram predictions. In *ICASSP*, pages 4779–4783, 2018.
- Kai Shen, Zeqian Ju, Xu Tan, Eric Liu, Yichong Leng, Lei He, Tao Qin, sheng zhao, and Jiang Bian. NaturalSpeech 2: Latent diffusion models are natural and zero-shot speech and singing synthesizers. In *The Twelfth International Conference on Learning Representations*, 2024.

- Hubert Siuzdak. Vocos: Closing the gap between time-domain and Fourier-based neural vocoders for high-quality audio synthesis. In *The Twelfth International Conference on Learning Representations*, 2024.
- Yakun Song, Zhuo Chen, Xiaofei Wang, Ziyang Ma, and Xie Chen. ELLA-V: Stable neural codec language modeling with alignment-guided sequence reordering. *arXiv preprint arXiv:2401.07333*, 2024.
- Keiichi Tokuda, Yoshihiko Nankaku, Tomoki Toda, Heiga Zen, Junichi Yamagishi, and Keiichiro Oura. Speech synthesis based on hidden Markov models. *Proceedings of the IEEE*, 101(5): 1234–1252, 2013.
- Hugo Touvron, Thibaut Lavril, Gautier Izacard, Xavier Martinet, Marie-Anne Lachaux, Timothée Lacroix, Baptiste Rozière, Naman Goyal, Eric Hambro, Faisal Azhar, et al. LLaMA: Open and efficient foundation language models. *arXiv preprint arXiv:2302.13971*, 2023.
- Apoorv Vyas, Bowen Shi, Matthew Le, Andros Tjandra, Yi-Chiao Wu, Baishan Guo, Jiemin Zhang, Xinyue Zhang, Robert Adkins, William Ngan, et al. Audiobox: Unified audio generation with natural language prompts. *arXiv preprint arXiv:2312.15821*, 2023.
- Chengyi Wang, Sanyuan Chen, Yu Wu, Ziqiang Zhang, Long Zhou, Shujie Liu, Zhuo Chen, Yanqing Liu, Huaming Wang, Jinyu Li, et al. Neural codec language models are zero-shot text to speech synthesizers. *arXiv preprint arXiv:2301.02111*, 2023.
- Yuxuan Wang, R.J. Skerry-Ryan, Daisy Stanton, Yonghui Wu, Ron J. Weiss, Navdeep Jaitly, Zongheng Yang, Ying Xiao, Zhifeng Chen, Samy Bengio, Quoc Le, Yannis Agiomyrgiannakis, Rob Clark, and Rif A. Saurous. Tacotron: Towards end-to-end speech synthesis. In *Proc. Interspeech 2017*, pages 4006–4010, 2017.
- Detai Xin, Xu Tan, Kai Shen, Zeqian Ju, Dongchao Yang, Yuancheng Wang, Shinnosuke Takamichi, Hiroshi Saruwatari, Shujie Liu, Jinyu Li, et al. RALL-E: Robust codec language modeling with chain-of-thought prompting for text-to-speech synthesis. *arXiv preprint arXiv:2404.03204*, 2024.
- Neil Zeghidour, Alejandro Luebs, Ahmed Omran, Jan Skoglund, and Marco Tagliasacchi. Soundstream: An end-to-end neural audio codec. *IEEE/ACM Transactions on Audio, Speech, and Language Processing*, 30:495–507, 2021.
- Heiga Zen, Andrew Senior, and Mike Schuster. Statistical parametric speech synthesis using deep neural networks. In *2013 IEEE international conference on acoustics, speech and signal processing*, pages 7962–7966, 2013.
- Heiga Zen, Viet Dang, Rob Clark, Yu Zhang, Ron J Weiss, Ye Jia, Zhifeng Chen, and Yonghui Wu. LibriTTS: A corpus derived from librispeech for text-to-speech. *arXiv preprint arXiv:1904.02882*, 2019.
- Ziqiang Zhang, Long Zhou, Chengyi Wang, Sanyuan Chen, Yu Wu, Shujie Liu, Zhuo Chen, Yanqing Liu, Huaming Wang, Jinyu Li, et al. Speak foreign languages with your own voice: Cross-lingual neural codec language modeling. *arXiv preprint arXiv:2303.03926*, 2023.

A Appendix

A.1 Derivation of Kullback-Leibler (KL) Divergence Loss

We assume that \mathbf{z}_t follows a multivariate Gaussian distribution where each dimension is independent. Combining equation (5), the KL divergence loss among T time steps can be analytically computed as

$$\begin{aligned}
\mathcal{L}_{\text{KL}}(\mathbf{y}, \mathbf{z}) &= \sum_{t=0}^{T-1} D_{\text{KL}}(p_{\theta}(\mathbf{z}_t | \mathbf{e}_t) \| p(\mathbf{z}_t)) \\
&= \sum_{t=0}^{T-1} D_{\text{KL}}(\mathcal{N}(\boldsymbol{\mu}_t, \text{diag}(\boldsymbol{\sigma}_t^2)) \| \mathcal{N}(\mathbf{y}_t, \mathbf{I})) \\
&= \sum_{t=0}^{T-1} \sum_{i=1}^d \int \frac{1}{\sqrt{2\pi\boldsymbol{\sigma}_t^2[i]}} e^{-\frac{(x-\boldsymbol{\mu}_t[i])^2}{2\boldsymbol{\sigma}_t^2[i]}} \log \frac{e^{-(x-\boldsymbol{\mu}_t[i])^2/2\boldsymbol{\sigma}_t^2[i]}/\sqrt{2\pi\boldsymbol{\sigma}_t^2[i]}}}{e^{-(x-\mathbf{y}_t[i])^2/2}/\sqrt{2\pi}} dx \\
&= \sum_{t=0}^{T-1} \sum_{i=1}^d \int \frac{1}{\sqrt{2\pi\boldsymbol{\sigma}_t^2[i]}} e^{-\frac{(x-\boldsymbol{\mu}_t[i])^2}{2\boldsymbol{\sigma}_t^2[i]}} \log \frac{e^{((x-\mathbf{y}_t[i])^2 - (x-\boldsymbol{\mu}_t[i])^2/\boldsymbol{\sigma}_t^2[i])/2}}}{\sqrt{\boldsymbol{\sigma}_t^2[i]}} dx \\
&= \frac{1}{2} \sum_{t=0}^{T-1} \sum_{i=1}^d \int \frac{1}{\sqrt{2\pi\boldsymbol{\sigma}_t^2[i]}} e^{-\frac{(x-\boldsymbol{\mu}_t[i])^2}{2\boldsymbol{\sigma}_t^2[i]}} ((x-\mathbf{y}_t[i])^2 - (x-\boldsymbol{\mu}_t[i])^2/\boldsymbol{\sigma}_t^2[i] - \log \boldsymbol{\sigma}_t^2[i]) dx \\
&= \frac{1}{2} \sum_{t=0}^{T-1} \sum_{i=1}^d \left(\int \frac{1}{\sqrt{2\pi\boldsymbol{\sigma}_t^2[i]}} e^{-\frac{(x-\boldsymbol{\mu}_t[i])^2}{2\boldsymbol{\sigma}_t^2[i]}} ((x-\boldsymbol{\mu}_t[i]) + (\boldsymbol{\mu}_t[i] - \mathbf{y}_t[i]))^2 dx \right) - 1 - \log \boldsymbol{\sigma}_t^2[i] \\
&= \frac{1}{2} \sum_{t=0}^{T-1} \sum_{i=1}^d (\boldsymbol{\sigma}_t^2[i] + (\boldsymbol{\mu}_t[i] - \mathbf{y}_t[i])^2 - 1 - \log \boldsymbol{\sigma}_t^2[i]) \tag{10}
\end{aligned}$$

where d is the dimensionality of the feature space.

A.2 Mel-Spectrogram Extraction Protocol

We extract log-magnitude mel spectrograms from resampled 16 kHz audios as the target continuous speech representation throughout this work. To extract mel-spectrograms, we apply a 1024-point short-time Fourier transform (STFT) using the Hann window function, with a window length of 1024 and a hop length of 256. We then apply an 80-dimensional mel-filter with the frequency range of 80 Hz to 7600 Hz. Finally, we take the base-10 logarithm of the resulting output as the final acoustic representation.